UC Davis
UC Davis Previously Published Works

Title
Assessment of Weld Residual Stress Measurement Precision: Mock-Up Design and Results for the Contour Method

Permalink
https://escholarship.org/uc/item/39q452n5

Journal
Journal of Nuclear Engineering and Radiation Science, 1(3)

ISSN
2332-8983

Authors
Olson, Mitchell D
Hill, Michael R
Willis, Eric
et al.

Publication Date
2015-07-01

DOI
10.1115/1.4029413

Peer reviewed

eScholarship.org Powered by the California Digital Library
University of California

Assessment of Weld Residual Stress Measurement Precision: Mock-Up Design and Results for the Contour Method

Mitchell D. Olson[1], Michael R. Hill[1*], Eric Willis[2], Artie G. Peterson[3], Vipul I. Patel[4], Ondrej Muránsky[4]

[1] *Department of Mechanical and Aerospace Engineering, University of California, One Shields Avenue, Davis, CA 95616*

[2] *Electric Power Research Institute, 3420 Hillview Avenue, Palo Alto, CA 94304*

[3] *Electric Power Research Institute, 1300 Harris Blvd. Charlotte, NC 28227*

[4] *ANSTO, Institute of Materials Engineering, New Illawarra Road, Lucas Heights, NSW, 2234, Australia*

Submitted to Journal of Nuclear Engineering and Radiation Science, October, 2014
Accepted for publication, December 2014.

ABSTRACT

Recent experimental work has shown residual stress measurements in welded material to be difficult. To better assess the precision of residual stress measurement techniques, a measurement article was designed to allow repeat measurements of a nominally identical stress field. The measurement article is a long 316L stainless steel plate containing a machine controlled eight-pass slot weld. Measurements of weld direction residual stress made with the contour method found high tensile stress in the weld and heat affected zone, with a maximum near 450 MPa and compressive stress away from the weld, a typical residual stress profile for constrained welds. The repeatability standard deviation of repeated contour method residual stress measurements was found to be less than 20 MPa at most spatial locations away from the boundaries of the plate. The repeatability data in the weld are consistent with those from a previous repeatability experiment using the contour method in quenched aluminum bars. A finite element simulation and neutron diffraction measurements were performed for the same weld and provided results consistent with the contour method measurements. Much of the material used in the work remains available for use in assessing other residual stress measurement techniques, or for an interlaboratory reproducibility study of the contour method.

Keywords: Residual stress, welding, repeatability, contour method, neutron diffraction, computational weld modeling

1. INTRODUCTION

Nuclear power plants have several important welds connecting pressure vessels to piping [1]. One such connection is a pressurizer safety/relief nozzle that connects a low alloy steel pressurizer to stainless steel piping [2]. Typically, the pressurizer nozzle is welded to a stainless steel "safe end" with a nickel alloy weld, and then the safe end is welded to stainless steel piping with a stainless steel weld.

* Corresponding author. Tel.: 530-754-6178; fax: 530-752-4158.
E-mail address: mrhill@ucdavis.edu

Welding causes cyclic thermomechanical deformation, and residual stress [3], and welding induced residual stress can be highly tensile, with magnitude approaching yield strength [4].

Tensile weld residual stresses have consequences on long term material performance and structural integrity, particularly relative to the rates of subcritical crack growth driven by cyclic loading or corrosion. Nuclear power plant fleet management decisions and design are informed by residual stress information, and the aging of current plants has driven research to develop additional weld residual stress data. The need for such research is due to the difficulty of residual stress measurements in certain nuclear power plant piping welds, known as dissimilar metal (DM) welds, which typically have relatively large thickness (more than 25 mm), cylindrical geometry, and complex material condition (microstructure with large grains, multiple phases, and preferred orientations). Ongoing efforts are directed to improving measurement and modeling methods for nuclear weld residual stress [5-9]. For example, measurements in a pressurizer safety/relief nozzle DM weld have been carried out, but were shown to be difficult, with comparisons between different measurement techniques showing the need for improvement of measurement techniques [10, 11]. While the eventual goal of such research is to assess residual stress in complex geometries like those present in nuclear power plants, here we take a preliminary step of assessing residual stress and measurement precision in a simpler geometry with limited experimental complexity. Earlier work suggests care is needed in the design of welded test articles, and here we build on earlier residual stress measurement studies.

Recently, an extensive research program for welding residual stress was undertaken by the Electric Power Research Institute (EPRI) and the United States Nuclear Regulatory Commission (NRC), working cooperatively under a memorandum of understanding [12]. The EPRI/NRC weld residual stress program included four phases. Each phase considered residual stresses as determined from model outputs and measurement data. Early phases used simplified articles, and later phases more complex

articles. The purpose of Phase 1 was to compare a range of residual stress measurement techniques and modeling approaches, in a number of highly controlled and relatively simple weld geometries. There were two types of Phase 1 measurement articles: welded plates and welded cylinders. The scope of Phase 1 included assessment of residual stresses over a range of welding configurations, so within each specimen type there are articles with different numbers of weld passes (for the plates) and weld materials (for the cylinders). The Phase 1 plates were manufactured in a fixture containing a backing plate to restrain the plate during welding (Fig. 1) and measurements were made while the plate was in the fixture, which complicated the measurements. There were limited opportunities to compare different measurement techniques on the same (or nominally identical) Phase 1 plates, but the limited comparisons that were made showed significantly different residual stress fields from what were expected to be complementary measurement techniques. Without data from repeated measurements on nominally identical articles, it was unknown whether the differences in measured residual stress were systematic or stochastic. One important observation from the Phase 1 work was that mechanical stress release methods, such as the contour method and the deep hole drilling method, showed promise for through-thickness residual stress measurements in welded articles. The present work built upon lessons learned in Phase 1 of the EPRI/NRC weld residual stress program and focuses on the creation of a high quality test article to be used to determine the precision of residual stress measurements.

The precision of a measurement technique can be assessed through a repeatability experiment [13] and quantified by the repeatability standard deviation, which is defined as the standard deviation of a given measurand obtained under repeatability conditions. Repeatability conditions are where independent test results are obtained with the same method on identical test items, in the same laboratory, by the same operator, using the same equipment, in short intervals of time. However, since residual stress measurements often change the residual stress state in the course of measurement, it is not usually possible to test identical items. Therefore, a sample is needed for assessing residual stress

measurement repeatability that has a degree of stress field uniformity that allows for a number of individual measurements of nearly identical residual stress.

The first goal of this work is to design a test article that has a stress field nominally constant at several planes, which enables a repeatability study for the contour method. Ideally, the article would have geometry that allows it to be sectioned into several smaller articles, that all have the same stress field. To meet this need, we describe the design of a long, continuously welded plate. The second goal of this work is to determine the precision of the contour method when measuring weld residual stress. Conveniently, the contour measurements can be performed while sectioning the long continuous weld into several nominally identical welded coupons. After fulfilling the two goals of the present work, the set of smaller coupons can be used for subsequent residual stress characterization and precision studies.

2. METHODS

The test article used in the present work was designed using the EPRI/NRC Phase 1 plate geometry as a starting point, with four significant changes. First, the plate was chosen to be thicker with a shallower weld groove so that the weld residual stress reflects a highly constrained, multi-pass weld, as typical of nuclear power plant DM welds. The geometry of the plates used here and in Phase 1 are compared in Fig. 2. The present plate is 25.4 mm (1 in) thick and 152.4 mm (6 in) wide, with a 6.35 mm (0.25 in) deep groove, to be filled in with a multi-pass weld. Relative to the Phase 1 design, the new sample has greater bending stiffness due to the additional material below the groove, which serves to elevate weld restraint and increase residual stress. The second change was to use stainless steel for both the plate (316L) and weld filler metal (308L), with material properties in Table 1. The third change was to increase the length of the plate to 1.22 m (48 in), to provide a long, continuous weld that can be sectioned into several smaller coupons for subsequent evaluation. This approach provides the

opportunity to develop a rich data set, where many measurements could be performed and compared on nominally identically coupons.

The fourth change simplified the restraint fixture, with measurements to be made after the restraint is removed. The new weld was restrained during fabrication by tack welding the plate to a large, stiff I-beam. The I-beam had a height and width of 203.2 mm (8 in), web thickness of 10.8 mm (0.44 in), and flange thickness of 11.2 mm (0.43 in). The tack welds were 9.5 mm (3/8 in) fillet welds, with complete welds along the 152.4 mm (6 in) ends of the plate, and seven equally spaced tack welds along the 1.22 m (48 in) edges, each 50.8 mm (2 in) long with a center-to-center pitch of 143.9 mm (5.667 in). The plate tack welded to the I-beam is shown in Fig. 3. As will be shown later, the choice to use intermittent tack welds for restraint was ill conceived, because it created some variation of stress along the weld length, and a continuous tack weld or no constraint weld would have been a better choice. After welding was complete, the tack welds were ground off, so that the plate was free from the I-beam, which simplified residual stress measurements.

The continuous weld was made with eight passes using machine controlled gas tungsten arc welding (GTAW), using the weld bead sequence in Fig. 4. To fully document the weld process, various data were recorded during fabrication including voltage, current, electrode travel speed, and wire feed rate. Each weld pass was staggered with 19 mm (0.75 in) spacing between beads, so the evolution of the weld bead geometry could be discerned (Fig. 5). Strain and temperature were recorded for each pass at multiple locations as a function of time and GTAW tungsten electrode location. A dimensioned drawing of the strain gage locations is shown in Fig. 6a, thermocouple locations are shown in Fig. 6b, and a photograph of the gages and thermocouples as installed on the plate can be seen in Fig. 7. Weld condition and process data are useful for documentation, but also for defining inputs to a computational weld simulation that can provide a numerical estimate of residual stress in the plate; a paper on a

companion simulation of this weld appears elsewhere [14], and simulation outputs are compared to measured residual stress below.

After completing the multi-pass groove weld, the tack welds were ground off, and the ends of the plate removed so that the remaining length was 762 mm (30 in), with 304.8 mm (12 in) removed from the end where each weld pass started, containing the "staggered" welds, and 152.4 mm (6 in) removed from the end where each weld pass stopped. The ends were removed to discard material having a stress state affected by the start and stop of welding. Eight samples were taken from the end containing the staggered passes, one sample near the middle of each staggered section. These samples were mounted and etched to characterize the geometry of each weld pass, including the bead and heat affected zone shapes, which also serve as input to weld simulation.

Contour method measurements were made at five planes along the plate length to characterize the residual stress field in the plate, and simultaneously to cut it into a set of nearly identical smaller samples. The first contour measurement was at the center of the plate (plane 1 in Fig. 8), followed by measurements at the center of the remaining half plates (planes 2A, 2B), and finally by two measurements at the center of two quarter plates (planes 3A, 3B). Analysis of results from the five measurements provides information on the consistency of the residual stress along the plate length, and assuming the stress is uniform with length, an estimate of contour method measurement precision.

The contour method was established by Prime [15]. He noted that when a part containing residual stress is cut in two on a plane of interest, cut-plane deformations occur due to the release of residual stress. By measuring the out-of-plane displacements at the cut face, a two-dimensional map of the out-of-plane residual stress can be found by forcing the displacements back to their original position (i.e., a flat plane) in a finite element model. The experimental steps of the contour method have been detailed in [16], and a summary of the technique is provided here.

For each contour measurement on the weld, the plate was securely clamped and then cut on the measurement plane using a wire electric discharge machine (EDM). The deformed surface of each side of the measurement plane was measured with a laser scanning profilometer along the cross-section with a measurement spacing of 100 μm in the thickness direction and 200 μm in the width direction, so that there were roughly 190,000 data points for each surface. Both sides of the cut surface are averaged on a common grid, and the average surface is fit with a smooth bivariate Fourier series [17]. A level of smoothing is determined by choosing fitting parameters during data reduction. The choice of fitting parameters, (m, n), determines the number of terms in the bivariate Fourier series, where the number of terms in the width direction is determined by m and the in the thickness direction by n.

The residual stress on the measurement plane was found by applying the negative of the smoothed deformation profile as a displacement boundary condition in a linearly elastic finite element model of the plate. The finite element mesh used eight-node linear displacement brick elements, with node spacing of approximately 1 mm on the cross-section in both in-plane directions. There were three different models, corresponding to the part configurations after cut 1, cut 2A and 2B, and 3A and 3B, each model having a length that corresponded to the pre-cut geometry. All three models had small (1 mm) node spacing along the length direction at the cut plane and larger node spacing at the opposite end, being 8 mm, 6 mm, and 4 mm in the three models (larger free-end spacing for longer models). The three models had a total number of elements of 460,000 (cut 1), 295,000 (cuts 2A and 2B), and 180,000 (cuts 3A and 3B). The material properties used in the analysis were elastic modulus of 206 GPa and Poisson's ratio of 0.3 [9]. Output from the finite element model provided the measured residual stress on the cut plane.

The average and repeatability standard deviation of the measured population were found as a function of in-plane position. The repeatability standard deviation was calculated as

$$s(x,y) = \sqrt{\frac{1}{N-1}\sum_{i=1}^{N}\left(\sigma_i(x,y) - \bar{\sigma}(x,y)\right)^2} \quad (1)$$

where, $s(x, y)$ is the repeatability standard deviation at a given in-plane position (x, y), N is the number of measurements, $\sigma_i(x, y)$ is the measured stress at (x, y) in the *ith* measurement, and $\bar{\sigma}(x, y)$ is the mean measured stress at (x, y) [18].

For each contour measurement, there is the possibility of stress redistribution due to the free surface created during a prior measurement, and the measurement should be corrected to account for that effect. A prior measurement causes stress redistribution that is largest at the cut plane (total release), and decays with distance from the cut plane, being negligible at some distance. When measurement planes are close together, a prior measurement will significantly affect stress found in a subsequent measurement. Earlier work has shown that results from a prior measurement can be used to "correct" the subsequent measurement [19-21]. The correction comprises an elastic stress analysis that estimates stress relaxation at the subsequent plane due to stress determined by the prior measurement. For the contour method, the correction for prior measurement is particularly convenient, having been determined during the required stress analysis step. The correction for contour, then, simply amounts to using the stress calculated in the typical the contour method finite element analysis, for the prior measurement, and extracting results along the plane of the subsequent measurement.

3. RESULTS

Basic data collected during and following weld fabrication are shown in Table 2 and weld bead profiles can be seen in the micrographs of Fig. 9. The micrographs show the evolution of the weld as new weld beads are applied. Axial strain and temperature data can be seen in Fig. 10, for the first weld pass, as a function of the GTAW tungsten electrode location along the length of the plate. Data for this

weld pass, as well as all others (not reported here for brevity), were used as input and calibration data for the companion weld simulation [22].

The two surface profiles from contour cut 1 can be seen in Fig. 11 (a and b). Both surface profiles show negative displacements near the weld, which is consistent with release of tensile weld residual stress. Both profiles have similar shape, suggesting that the part was properly constrained during cutting. The average surface profile (Fig. 11c) was fit to a bivariate Fourier series with parameters $m = 6$ and $n = 2$, giving the profile in Fig. 11d. Line plots of the surface profiles can be seen in Fig. 12, which show the fit surface following the trend in the data while ignoring noise. Surface profile fits for contour measurements at other planes used the same fitting parameters, $m = 6$ and $n = 2$.

During the contour measurement at cut 2A, the EDM wire broke at 10 mm from the weld center, possibly due to the wire contacting a non-conductive inclusion. To proceed with the measurement, the part was cut from the opposite side (i.e., cut from $x = 76.2$ mm to $x = 10$ mm). Cutting in this manner caused a significant "step" in the average surface profile, as can be seen in Fig. 13. Clearly, the data around the wire break are erroneous and were removed during data processing, but the measurement remained an outlier, and results from plane 2A were discarded.

The results of the remaining contour measurements can be seen in Fig. 14. The results show high tensile stress in the weld region, with a maximum near 450 MPa, giving way to nearby low magnitude compressive stresses (around -100 MPa), which is typical weld residual stress [23-25]. However, the results also show an area of larger compressive stress (about -250 MPa) toward the transverse edges, which was not expected, and may have been introduced during plate manufacture, prior to welding. Planes 3A and 3B are near the mid-length of the intermittent tack weld locations, while planes 1 and 2A fell between tack welds, and the results show large tensile stresses near the bottom of the transverse

edges at planes 3A and 3B that are absent at planes 1 and 2A. The difference in stress state appears mostly limited to an area within one plate thickness (25.4 mm) of the transverse edges.

To assess whether the residual stress state is constant along the length of the plate, the stress at middle of the weld ($x = 0$) is plotted versus position along the length for several vertical positions ($y = 5$, 10, 15, and 20 mm) in Fig. 15. The results show the stress is nominally consistent along the length of the plate. The stresses at planes 3A and 3B are somewhat different than at planes 1 and 2B, which we suspect is due to their position relative to the intermittent tack welds, which are indicated on the figure. Even with these differences, we conclude that measured residual stress is consistent along the plate, and each of the sections produced by the contour cuts may be assumed identical in further work.

The mean measured residual stress and repeatability standard deviation are given in Fig. 16. The mean is similar to each individual measurement with tensile stress in the weld and compressive stress toward the transverse edges. The repeatability standard deviation is under 20 MPa over a large portion of the cross-section, but is near 30 MPa in the weld. A repeatability study assumes that measurements are made on articles with the same stress field and clearly that is not the case near the transverse edges, because some measurements cut through tack welds were and others did not. Therefore, repeatability standard deviation within one plate thickness of the transverse edges is omitted.

Line plots of the mean, repeatability standard deviation, and individual contour measurements allow more quantitative observation (Fig. 17). The line plot in the horizontal direction is at a vertical position of 17 mm (crosses the weld) and shows that the measurements are within a 35 MPa band around the mean for all locations. At ±15 mm from the weld center all measurements are within a few MPa. The line plot in the vertical direction at the weld center shows that the measurements are close to one another for the bottom 10 mm of the plate (within 20 MPa), but have somewhat more scatter toward the top of the weld, having a spread of around 50 MPa.

4. DISCUSSION

The level of contour method repeatability found here is consistent with a previous repeatability study [19] using quenched aluminum bars of rectangular cross-section. The results of the previous study had repeatability standard deviation between 5 and 10 MPa about 5 mm away from part boundary and up to 20 MPa at the part boundary. Here, the repeatability standard deviation is somewhat higher, but still relatively small away from the boundary, being under 20 MPa over most of the cross-section, and higher in the weld metal, with repeatability standard deviation of about 30 MPa. The higher repeatability standard deviation away from the boundary is consistent with the higher elastic modulus of the stainless steel relative to the aluminum in the prior study. But, because welding is generally more stochastic than quenching, and observed measurement precision is limited by true variations of the unknown residual stress, the higher repeatability standard deviation in the weld might be expected.

Measurements at planes 3A and 3B needed corrections because of their proximity to prior measurement planes, as discussed above. The correction at plane 3B from the measurement at plane 1 is shown in Fig. 18. The correction is roughly constant through-thickness and varies smoothly across the weld, being tensile at the weld center (20 MPa) and compressive at the transverse edges (-20 MPa). While the correction is small, relative to the total residual stress, it is significant relative to the repeatability standard deviation, and was therefore important to include. Corrections at plane 3A are very similar to that at plane 3B (Fig. 18).

To validate the measured residual stress, a weld simulation was performed [22] and a complementary measurement was made. To summarize the weld simulation, the model used sequentially coupled thermo-mechanical analysis carried out using finite element techniques. The heat source was calibrated using thermocouple data (Fig. 10) and the fusion zones of each weld pass that were identified from optical macrographs (Fig. 9). Complementary neutron diffraction measurements

were made at plane 3C (Fig. 8) using standard methodologies [26], and a companion paper details the experiment [27]. Line plots of the measurements and simulation output can be seen in Fig. 19. The horizontal line plot at y = 17 mm in Fig. 19a, shows all three to have very good agreement around the weld, but the contour method and weld simulation disagree near the transverse edges, likely due to the stress state present in the plate prior to welding. The vertical line plot at the weld center, in Fig. 19b, shows all data in general agreement, but the neutron diffraction results differ significantly (>100 MPa) at some locations; such point wise dispersion in neutron diffraction data is not uncommon, especially for welds due to the large grain size of the weld metal [28]. In summary, there is good agreement between the results of the contour method, neutron diffraction, and weld simulation, which gives confidence that the contour repeatability measurements are sound.

The repeatability standard deviation should be consistent with a useful single measurement uncertainty estimator [29], and recent work proposed a new single measurement uncertainty estimator for the contour method [30]. To compare the results of that estimator to the present repeatability standard deviation (Fig. 16b), we apply the estimator to the plane 1 measurement. The two principal error sources accounted for by the uncertainty estimator are the error associated with noise in the displacement data (due to surface roughness inherent in EDM cuts and errors in measurement of the surface profile), called the displacement error, and the error associated with smoothing the surface, called the model error. The displacement error is found by repeatedly (5x) applying normally distributed noise to the surface profile, computing stress with the noisy displacements, then taking the standard deviation of the five resulting stress distributions. The model error is found by taking the standard deviation of the resulting stresses from different, "nearby", levels of smoothing. The total uncertainty in $\sigma_{zz}(x, y)$ is found by taking the root sum square of the two error sources

$$U_{zz,tot} = \sqrt{U_{zz,disp}^2 + U_{zz,model}^2} \tag{2}$$

where $U_{zz,tot}$ is the total uncertainty (in the longitudinal stress), $U_{zz,disp}$ is the displacement error (in the longitudinal stress), and $U_{zz,model}$ is the model error. The resulting uncertainty estimate for plane 1 (Fig. 20) is generally consistent with the repeatability standard deviation (Fig. 16b), but the uncertainty is somewhat larger than the repeatability near the cross-section boundaries. The good comparison between the computed uncertainty and the observed repeatability suggests that the uncertainty estimator provides a reasonable, if conservative, estimate of contour method precision.

Overall the test article design, comprising a long welded plate, provided a useful outcome. The machine controlled, multi-pass weld produced a consistent stress along the plate length, and plate constraint provided high magnitude stress typical of nuclear power plant applications [31]. Furthermore, care was taken to collect data needed for weld simulation (weld input parameters, temperature, strain, and weld bead cross sections). While the tack welds provided a good level of restraint, as well as a deterministic boundary condition amenable to weld modeling, their intermittent placement along the weld introduced some inconsistency. Follow-on work should use restraint continuous along the length, or perhaps eliminate the restraint altogether.

5. SUMMARY/CONCLUSIONS

A welded article was designed to serve as the basis for a weld residual stress measurement repeatability study. Care was taken to design the article such that it would have constant stress along the length, to enable many locations for measuring the stress field independently, to use representative materials, to have a stress field typical of nuclear power plant piping welds, and to fully document the welding details for companion weld modeling. The welded article comprised a long stainless steel plate containing an eight-pass stainless steel slot weld.

Contour measurements were made as the plate was cut into smaller sections, and revealed high tensile stress in the weld region, with a maximum around 450 MPa, giving way to low magnitude

compressive residual stress (-100 MPa) further from the weld. Repeated measurements enabled assessment of the repeatability of the contour method, which was found to have repeatability standard deviation under 20 MPa at most spatial locations and around 30 MPa near the weld, excluding areas near the transverse edges that were affected by variability as a result of intermittent restraint welds. The contour measurement results were compared with results of neutron diffraction measurements and output from a weld simulation, with all three showing consistent residual stress.

6. ACKNOWLEDGEMENTS

The authors acknowledge the help of Mike Newman in fabricating the plate used in this study. The Electric Power Research Institute, Materials Reliability Program (Paul Crooker, Principal Technical Leader) provided financial support for this work.

REFERENCES

[1] S. H. Bush, "Failure mechanisms in nuclear power plant piping systems", *Journal of Pressure Vessel Technology,* vol. 114, pp. 389-395, 1992.

[2] P. Crooker and A. Csontos, "Cooperative Dissimilar Metal Butt-Weld Residual Stress Finite-Element Model Validation", 2010 Residual Stress Summit, Lake Tahoe, CA, USA, 2010.

[3] O. Muránsky, C. J. Hamelin, M. C. Smith, P. J. Bendeich, and L. Edwards, "The effect of plasticity theory on predicted residual stress fields in numerical weld analyses", *Computational Materials Science,* vol. 54, pp. 125-134, 2012.

[4] O. Muránsky, M. C. Smith, P. J. Bendeich, C. J. Hamelin, and J. M. Edwards, "Prediction and Measurement of Weld Residual Stresses in Thermally Aged Girth-Welded Austenitic Steel Pipes", PVP2012-78409, Proceedings of the ASME 2012 Pressure Vessels & Piping Division Conference, Toronto, Ontario, Canada, 2012.

[5] M. Kerr and H. J. Rathbun, "Summary of Finite Element (FE) Sensitivity Studies Conducted in Support of the NRC/EPRI Welding Residual Stress (WRS) Program", PVP2012-78883, in *ASME 2012 Pressure Vessels & Piping Division Conference*, Toronto, Ontario, Canada, 2012.

[6] C. R. Hubbard, "Neutron Diffraction Residual Strain Tensor Measurements Within the Phase IA Weld Mock-up Plate P-5", ORNL/TM-2011/304, Oak Ridge National Laboratory, 2011.

[7] C. R. Hubbard, "Neutron Diffraction Residual Stress Measurements withing the Phase III Nozzle S-3", ORNL/TM-2011/191, Oak Ridge National Laboratory, 2011.

[8] P. J. Bouchard, "Validated residual stress profiles for fracture assessments of stainless steel pipe girth welds", *International Journal of Pressure Vessels and Piping,* vol. 84, pp. 195-222, 2007.

[9] O. Muránsky, M. C. Smith, P. J. Bendeich, and L. Edwards, "Validated numerical analysis of residual stresses in Safety Relief Valve (SRV) nozzle mock-ups", *Computational Materials Science,* vol. 50, pp. 2203-2215, 2011.

[10] H. J. Rathbun, L. F. Fredette, P. M. Scott, A. A. Csontos, and D. L. Rudland, "NRC Welding Residual Stress Validation Program International Round Robin Program and Findings", PVP2011-57642, 2011 ASME Pressure Vessels & Piping Division Conference, Baltimore, MD, USA, 2011.

[11] L. F. Fredette, J. E. Broussard, M. Kerr, and H. J. Rathbun, "NRC/EPRI Welding Residual Stress Validation Program - Phase III Details and Findings", PVP2011-57645, ASME 2011 Pressure Vessels & Piping Division Conference, Baltimore, MD, USA, 2011.

[12] EPRI, "Materials Reliability Program: Finite-Element Model Validation for Dissimilar Metal Butt-Welds", MRP-316, Electric Power Research Institute, 2011.

[13] ASTM, "Standard Practice for Use of the Terms Precision and Bias in ASTM Test Methods", E177, ASTM International, West Conshohocken, PA, 2010

[14] V. I. Patel, O. Muránsky, C. J. Hamelin, M. D. Olson, M. R. Hill, and L. Edwards, "A Validated Numerical Model for Residual Stress Predictions in an Eight-Pass-Welded Stainless Steel Plate", Materials Science Forum, 2013.

[15] M. B. Prime and A. R. Gonzales, "The Contour Method: Simple 2-D Mapping of Residual Stresses", Sixth International Conference on Residual Stresses, Oxford, UK, 2000.

[16] F. Hosseinzadeh and P. J. Bouchard, "Application of the contour method to validate residual stress predictions", Second International Conference on Advances in Nuclear Materials (ANM- 2011), Mumbai, India, 2011.

[17] W. R. Thorpe, C. W. Rose, and R. W. Simpson, "Areal Intpolation of Rainfall with Double Fourier Series", *Journal of Hydrology,* vol. 42, pp. 171-177, 1979.

[18] H. W. Coleman and W. G. Steele, *Experimentation, Validation, and Uncertainty Analysis for Engineers*, Ch. 2, John Wiley & Sons, Inc., Hoboken, New Jersey, 2009

[19] M. R. Hill and M. D. Olson, "Repeatability of the Contour Method for Residual Stress Measurement", *Experimental Mechanics,* vol. 54, pp. 1269-1277, 2014.

[20] W. Wong and M. R. Hill, "Superposition and Destructive Residual Stress Measurements", *Experimental Mechanics,* vol. 53, pp. 339-344, 2013.

[21] P. Pagliaro, M. B. Prime, J. S. Robinson, B. Clausen, H. Swenson, M. Steinzig*, et al.*, "Measuring Inaccessible Residual Stresses Using Multiple Methods and Superposition", *Experimental Mechanics,* vol. 51, pp. 1123-1134, 2010.

[22] V. I. Patel, O. Muránsky, C. J. Hamelin, M. D. Olson, M. R. Hill, and L. Edwards, "Finite Element Modelling Of Welded Austenitic Stainless Steel Plate With 8-Passes", PVP2014-28209, ASME 2014 Pressure Vessels & Piping Division Conference, Anaheim, CA, USA, 2014.

[23] C. Ohms, R. C. Wimpory, D. E. Katsareas, and A. G. Youtsos, "NET TG1: Residual stress assessment by neutron diffraction and finite element modeling on a single bead weld on a steel plate", *International Journal of Pressure Vessels and Piping,* vol. 86, pp. 63-72, 2009.

[24] M. C. Smith and A. C. Smith, "NeT bead-on-plate round robin: Comparison of residual stress predictions and measurements", *International Journal of Pressure Vessels and Piping,* vol. 86, pp. 79-95, 2009.

[25] P. J. Bouchard, "The NeT bead-on-plate benchmark for weld residual stress simulation", *International Journal of Pressure Vessels and Piping,* vol. 86, pp. 31-42, 2009.

[26] ISO, "Non-destructive testing - Standard test method for determining residual stresses by neutron diffraction", ISO/TS 21432, International Organization for Standardization, 2005.

[27] M. D. Olson, M. R. Hill, V. I. Patel, O. Muránsky, and T. Sisneros, "Biaxial Residual Stress Mapping for a Stainless Steel Welded Plate", *Manuscript in preparation for publication in Pressure Vessel Technology,* 2014.

[28] O. Muránsky, M. Smith, P. Bendeich, T. Holden, V. Luzin, R. Martins*, et al.*, "Comprehensive numerical analysis of a three-pass bead-in-slot weld and its critical validation using neutron and synchrotron diffraction residual stress measurements", *International Journal of Solids and Structures,* vol. 49, pp. 1045-1062, 2012.

[29] P. R. Bevington and D. K. Robinson, "*Data reduction and error analysis for the physical sciences*", McGraw-Hill New York, 1969.

[30] M. D. Olson, A. T. DeWald, M. R. Hill, and M. B. Prime, "Contour Method Uncertainty Estimation", *Experimental Mechanics,* 2014.

[31] J. A. Francis, H. K. D. H. Bhadeshia, and P. J. Withers, "Welding residual stresses in ferritic power plant steels", *Materials Science and Technology,* vol. 23, pp. 1009-1020, 2007.

TABLES

Material	E (GPa)	ν	Yield Stress (MPa)
316L Stainless steel	206	0.30	440
308L Stainless steel	204	0.30	350

Table 1: Material properties

Pass Number	1	2	3	4	5	6	7	8
Primary Amp [A]	214.3	214.3	214.3	244.7	244.7	244.2	244.7	244.2
Background Amp [A]	163.8	164	164	183.9	184.4	183.4	183.9	183.9
Primary Voltage [V]	9.3	9.7	9.7	9.8	9.7	9.8	9.8	9.9
Background Voltage [V]	8.5	9	8.8	8.8	8.7	8.8	8.7	8.8
Primary Wire Feed [in/min]	40.3	40.3	40.3	59.8	60	60	60	60
Background Wire Feed [in/min]	33.0	33.0	33.2	52.6	52.8	52.6	52.6	52.8
Primary Travel [in/min]	4.5	4.5	4.5	4.5	4.5	4.5	4.5	4.5
Interpass Temperature [ºF]	120	145	157	181	192	196	214	218
Ambient Temperature [ºF]	72	72	72	72	72	72	72	72

Table 2: Welding Parameters

FIGURES

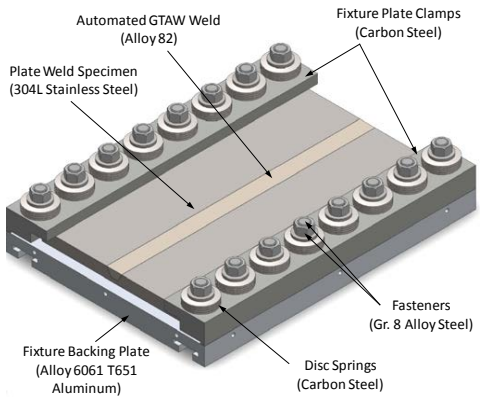

Fig. 1 – Phase 1 plate with restraint fixture. Reproduced from EPRI, MRP-316

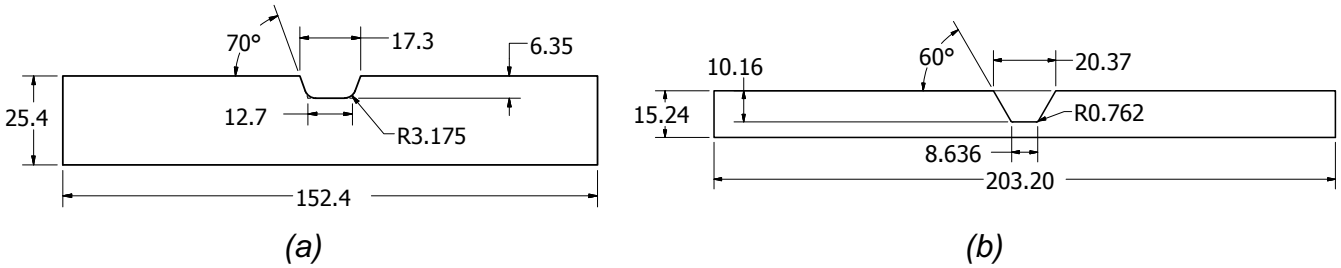

Fig. 2 – Dimensioned diagrams of plate cross-section with details of the machined weld groove used in (a) this work and (b) NRC/EPRI Phase 1. Dimensions in mm

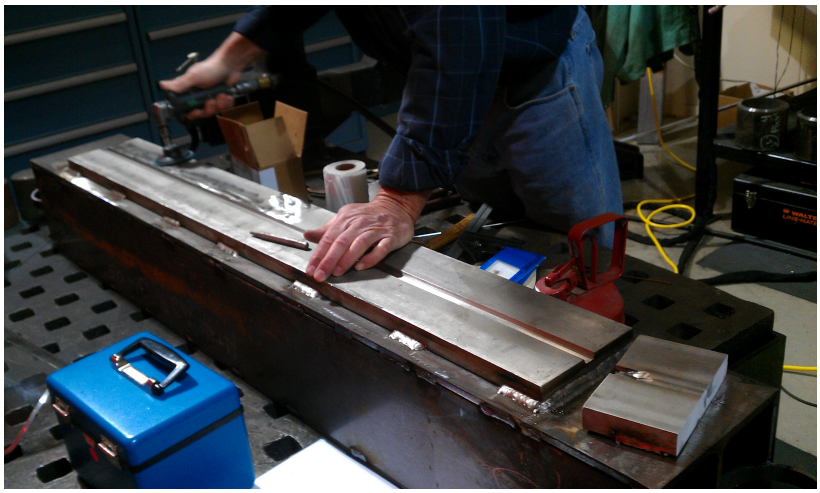

Fig. 3 – Plate on I-beam after completion of tack welds

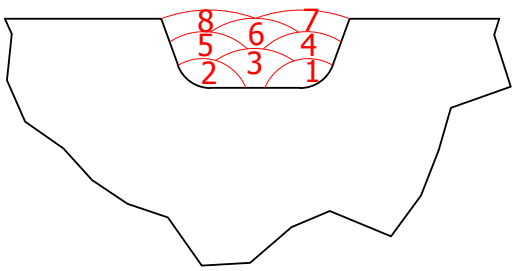

Fig. 4 – Weld bead order

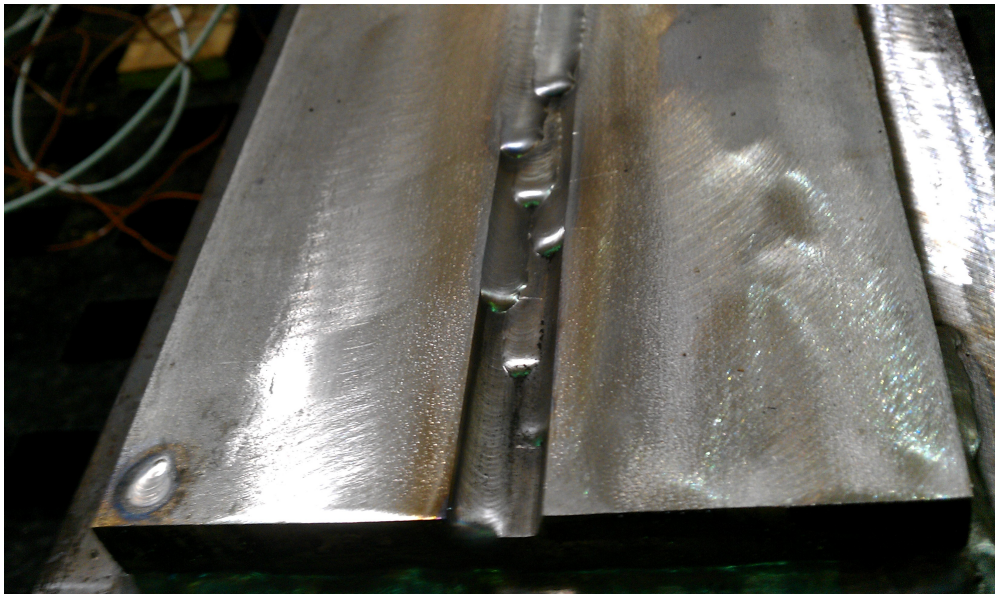

Fig. 5 –"Staggered" weld to determine weld bead geometry evolution with each weld pass

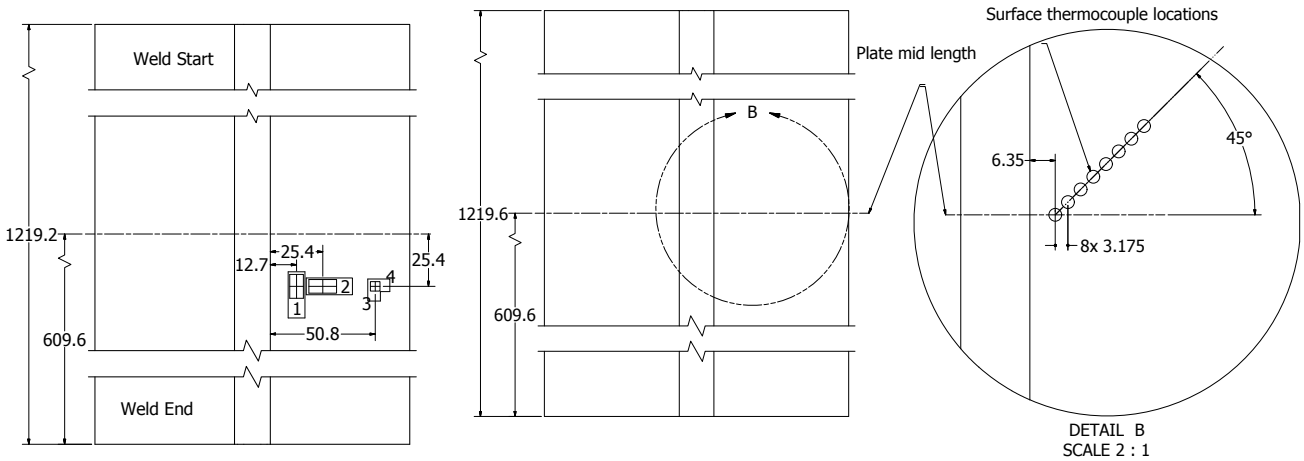

(a) (b)

Fig. 6 – Sensor locations for measurements during welding: (a) strain gages (1 and 3 are axial, 2 and 4 transverse), and (b) thermocouples. Dimensions in mm

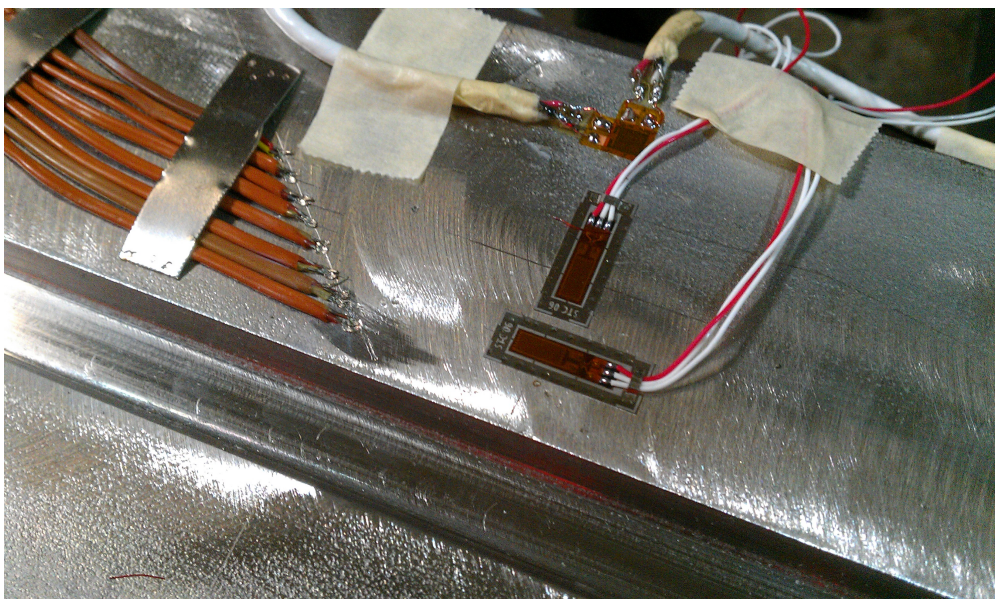

Fig. 7 – Strain gages and thermocouples used during welding

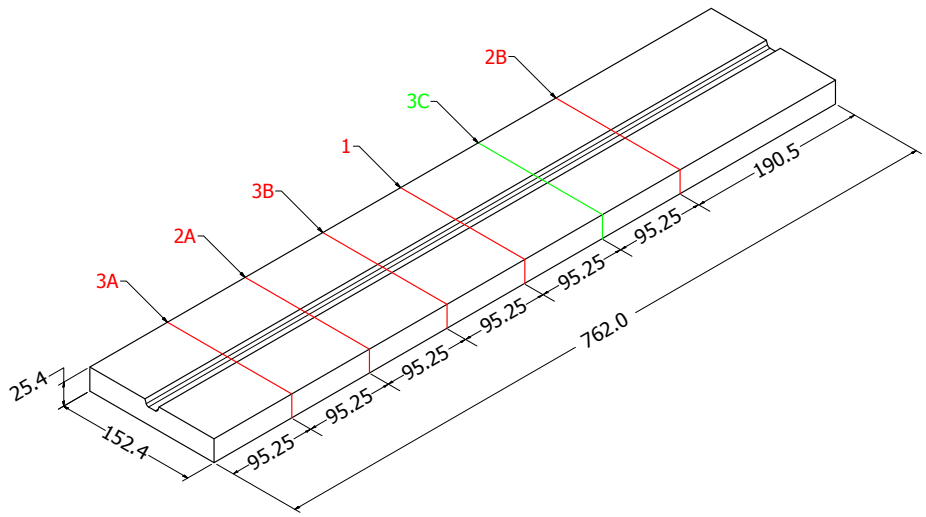

Fig. 8 – Measurement plane locations, with contour planes in red and the neutron diffraction plane in green. Dimensions in mm

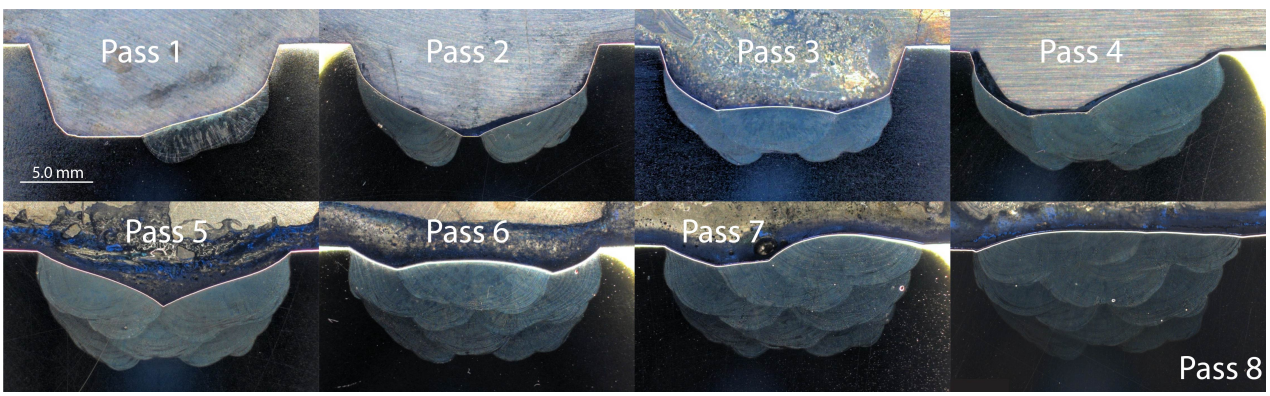

Fig. 9 – Evolution of weld bead geometry in the staggered weld

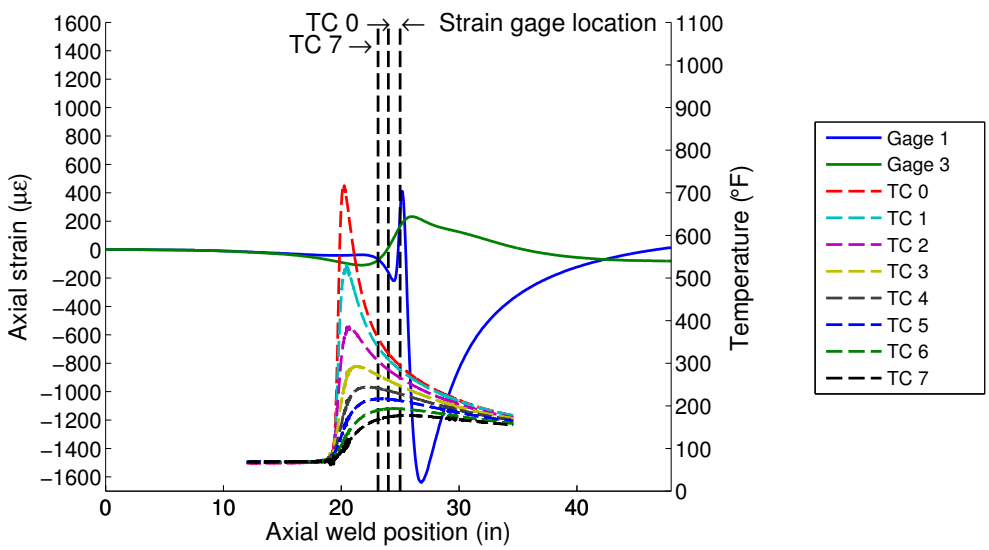

Fig. 10 – Axial strain and temperature for the first weld pass versus welding electrode position

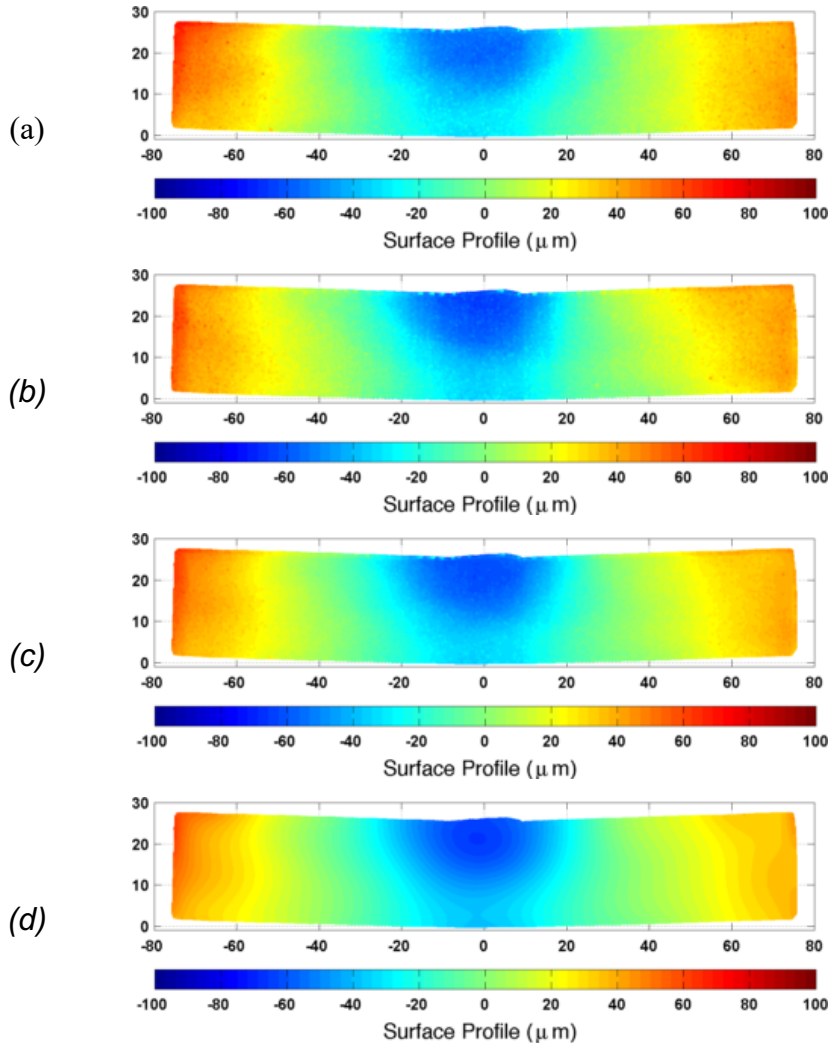

Fig. 11 – Surface profiles from contour measurement at plane 1: (a) surface 1, (b) surface 2, (c) average surface, and (d) fit surface

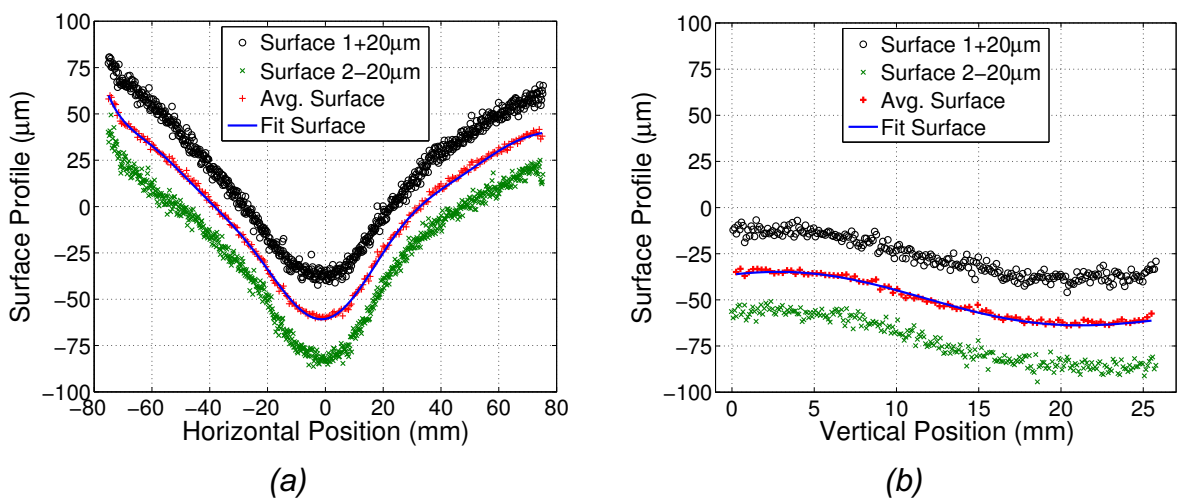

Fig. 12 – Line plots of the plane 1 surface profiles (20 μm added to surface 1 and 20 μm subtracted from surface 2), average surface, and fit surface from the contour measurement along: (a) horizontal direction at y = 17 mm and (b) along the vertical at the weld center (x = 0)

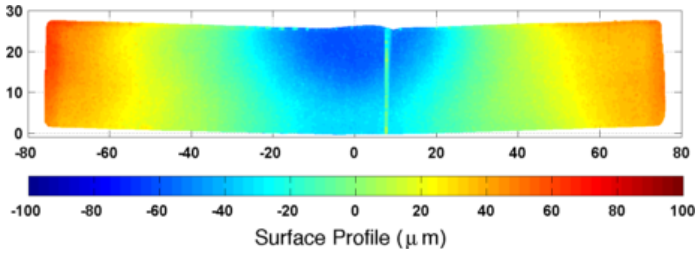

Fig. 13 – Average surface profile from contour measurement at plane 2A

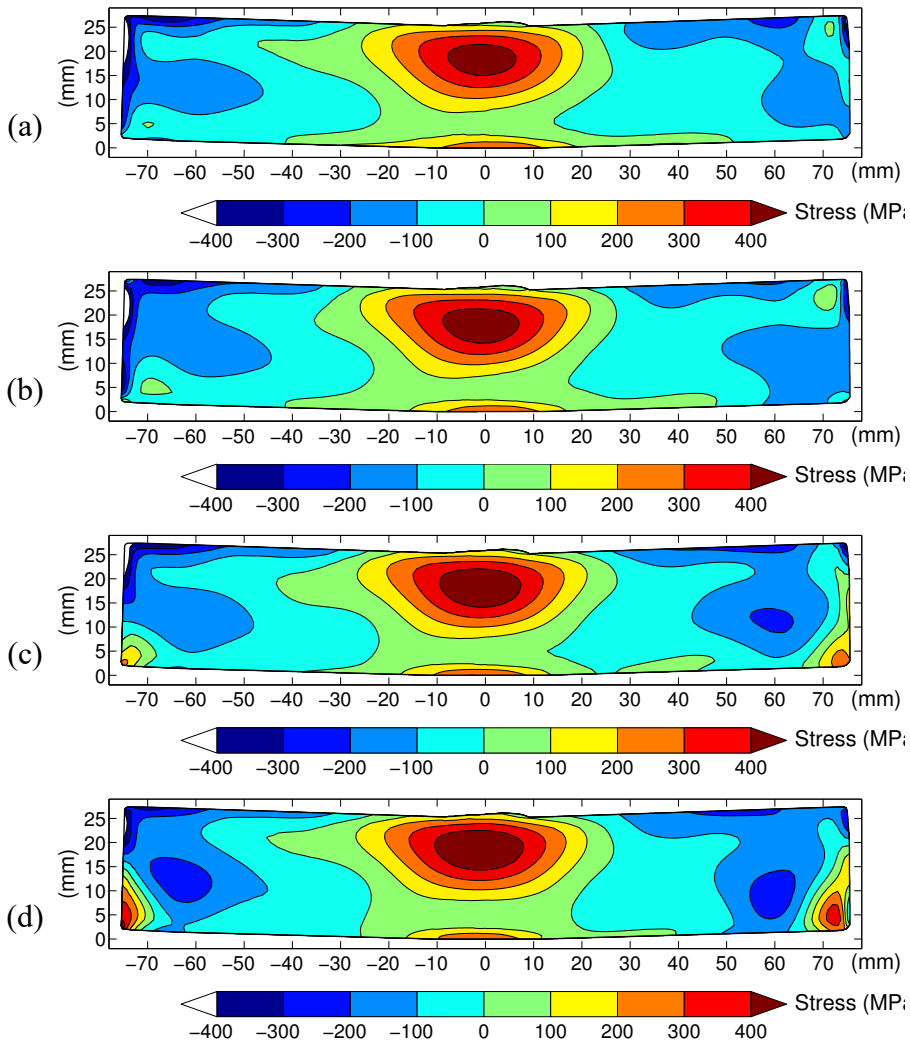

Fig. 14 – Contour measurement results at plane (a) 1, (b) 2B, (c) 3A, and (d) 3B

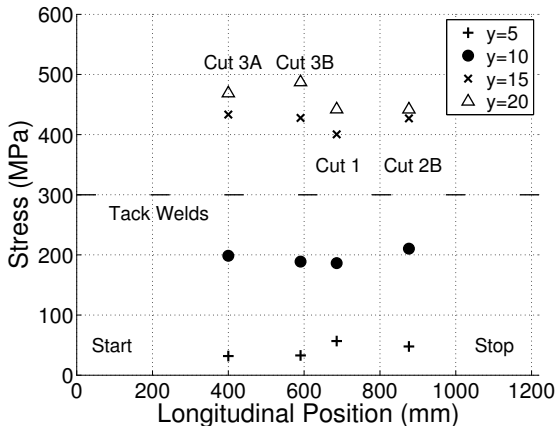

Fig. 15 – Plot of the longitudinal stresses at the weld center (x = 0) versus position along the weld length, at vertical positions of 5 mm, 10 mm, 15 mm, and 20 mm

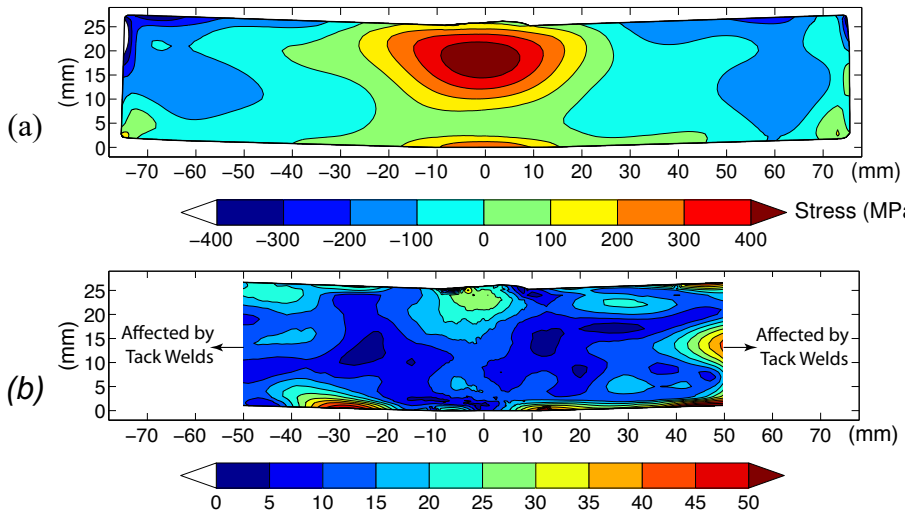

Fig. 16 – (a) Mean stress and (b) repeatability standard deviation of the four contour measurements

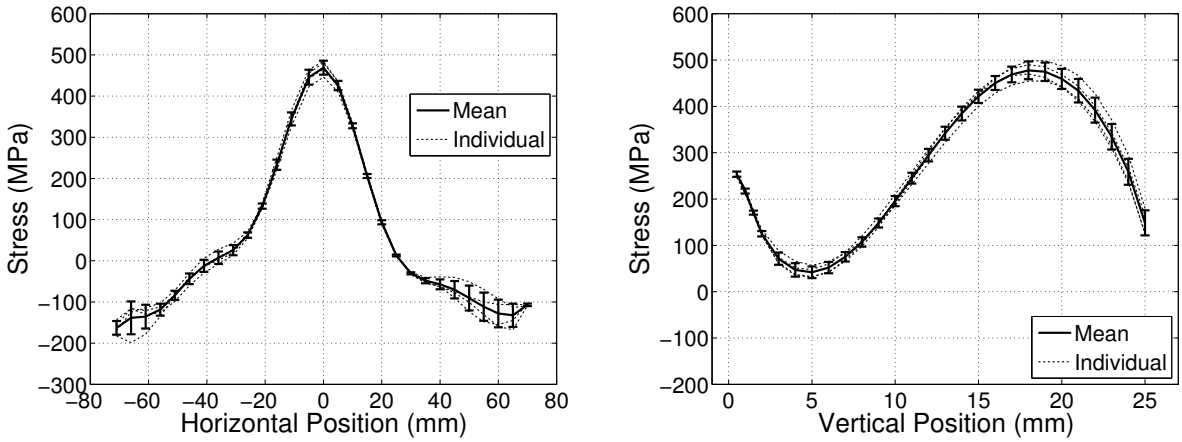

(a) *(b)*

Fig. 17 – Line plots of the mean (thick line), repeatability standard deviation (error bars), and individual measurements (dashed lines), along the (a) horizontal at y = 17 mm, and (b) vertical at the weld center (x = 0)

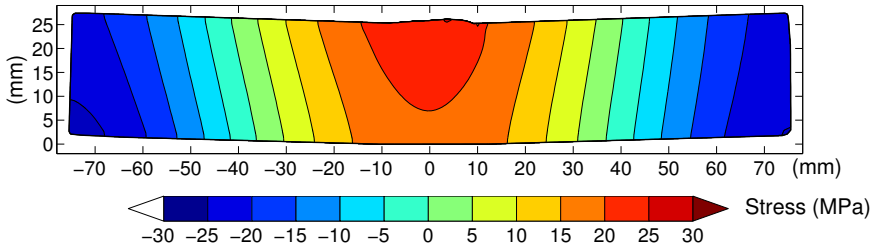

Fig. 18 – Correction at plane 3B from the contour measurement at plane 1

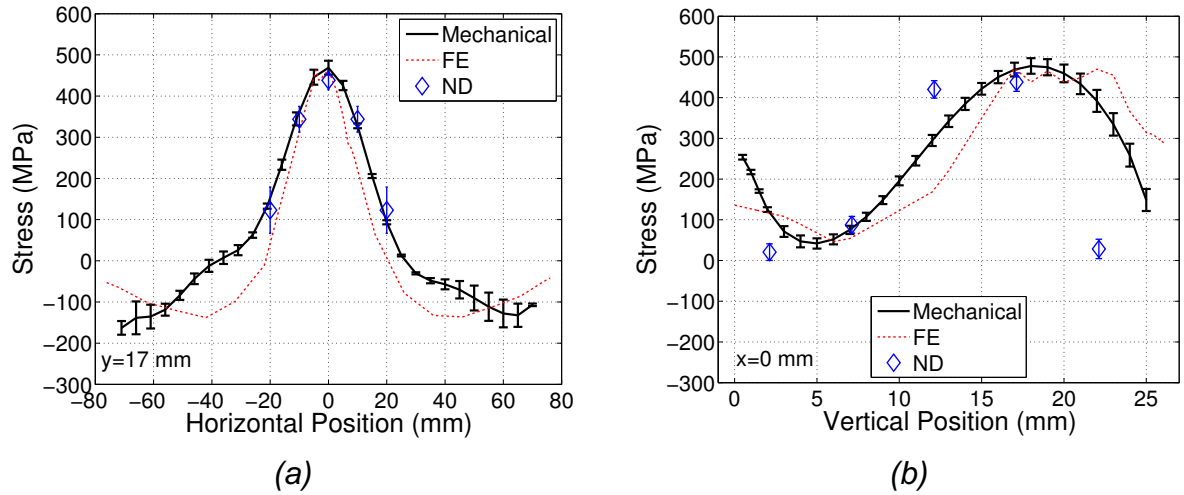

Fig. 19 – Line plots comparing the mean measured residual stress (Mechanical), with repeatability standard deviation shown as error bars, weld simulation output (FE), and neutron diffraction measurements (ND) along the (a) horizontal at y = 17 mm, and (b) vertical at the weld center (x = 0)

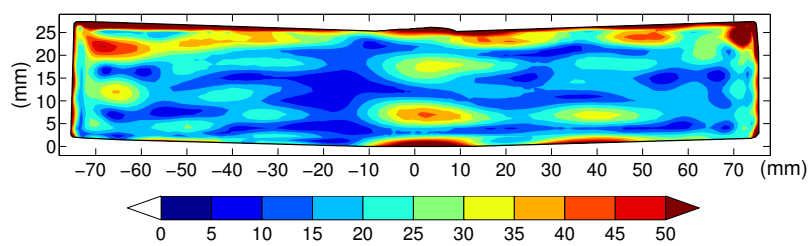

Fig. 20 – Uncertainty for the longitudinal stress (68% confidence interval)